ACS OMEGA

Open Access

http://pubs.acs.org/journal/acsodf

Article

EVQ-218: Characterization of High-Energy Nanoparticles that Measure up to NIST Standards

Bretni S. Kennon* and William H. Niedermeyer

Cite This: *ACS Omega* 2024, 9, 7891−7903

Read Online

ACCESS | Metrics & More | Article Recommendations | Supporting Information

ABSTRACT: EVQ-218 is a high-energy produced nanoparticle (NP) with a method of manufacture that avoids chemical or biological synthesis. The patented single-step process generates stable, pure metal NPs directly into HPLC grade water. Laser ablation via the multiple cross laser system occurs at a rate that is in the region of dielectric breakdown, generating temperatures and pressures akin to those of diamond formation. The spherical particles from this method have an ultrastable shell structure that inhibits the hallmark ion emission that occurs in other nanosilver species. The resulting particle size distribution is so narrow that additional size refinement or stabilizing chemistries are not necessary. These properties make EVQ-218 an attractive clean and green alternative to traditional nanosilvers, particularly when factoring in shelf life, as EVQ-218 maintains (uniform) stability for years, while NIST standard materials degrade within a few weeks. EVQ-218 characterization and differentiation are timely as the rise of antimicrobial resistance has caused a surge of research on antimicrobial silver NPs. It has been widely established that the antimicrobial activity of nanosilver is due to ion emission. Unfortunately, metal ions can be quite toxic and prevent certain biomedical and consumer product applications. In an ever-changing regulatory landscape, there is increasing scrutiny to definitively characterize nanomaterials and assess their potential environmental/toxicological footprint. EVQ-218 was characterized alongside comparable NIST standard NPs, with particular interest in speciation and fate. Particle characterization studies reveal that EVQ-218 is nearly equivalent to NIST standard material with respect to particle morphology and uniformity. Dissolution and surface chemistry studies quickly differentiate EVQ-218 as the first stable, nonemissive, pure metal NP that is on par with NIST standards for ideal materials.

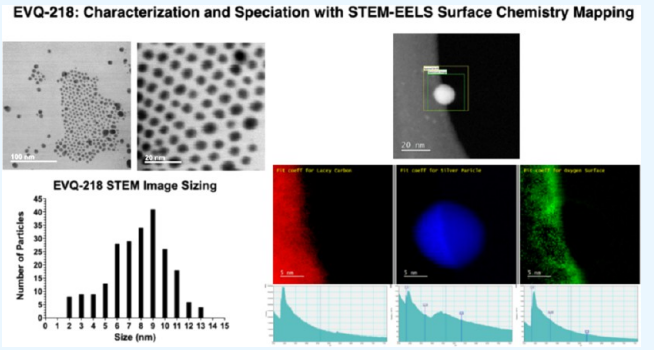

INTRODUCTION

Silver has been known for its antibacterial qualities for centuries.[1,2] Over the last few decades, nanosilver has experienced increasing interest as a functional material additive, with the number of studies and publications steadily rising. Countless products have incorporated nanosilver and other engineered nanomaterials[3−7] that exhibit antimicrobial activity. Studies show that antimicrobial activity is typically due to ion emission or reactive oxygen species, which are toxic to nonpathogenic organisms.[8−11] As a result, there has been enhanced scrutiny on the safety and regulation of nanosilver and similar antimicrobial nanoparticles (NPs).[4−6,12,13]

Silver nanoparticles (AgNPs) are produced in a variety of ways, including chemical synthesis, milling, ablation, and even biosynthesis using plants or pathogens.[14−20] Each method leads to different surface chemistry, emissivity, stability, and purity, resulting in different efficacy and toxicity.[9,21,22] Increased research emphasizing safety and fate has led to the issuance of many ASTM, ISO, and comparable regulatory level test guidelines to compare each new AgNP species to its nearest NIST analogue and silver ion. Of particular interest is the ionic content, particle uniformity, and stability/emissivity. It is critical to determine these properties for new NP species.

Nanomaterials research often involves surface-enhanced Raman behaviors. For decades, scientists have investigated SERS (surface-enhanced Raman spectroscopy) and other nanomaterial phenomena that can be harnessed for a wide variety of analytical techniques. EVQ-218 was born from similar pursuits, namely, creation of a more "ideal" NP, free from the surface coatings and stabilizers found in known analogous particles. Unfortunately, many of the top-down methods of making NPs do not yield desirable size distributions. Laser ablation was identified as a promising top-down method and leads to the development of EVQ-218 and the patented ATTOSTAT method of particle manufac-

Received: October 5, 2023
Revised: January 12, 2024
Accepted: January 19, 2024
Published: February 9, 2024

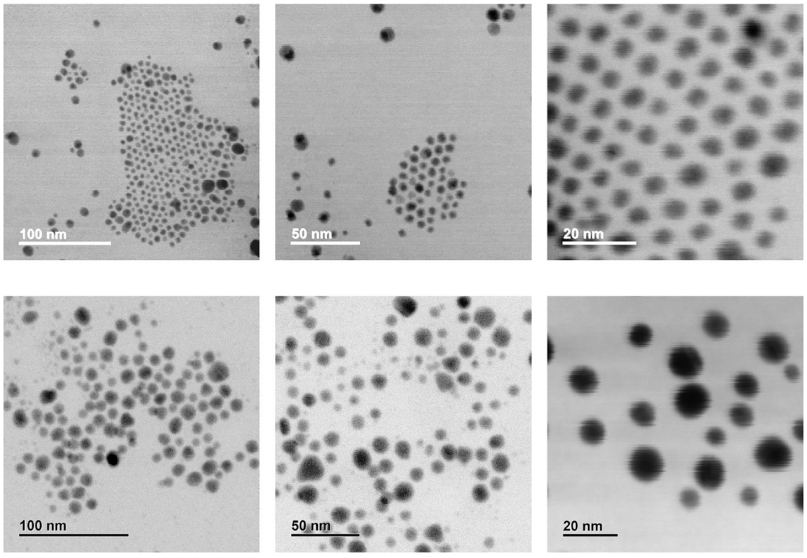

Figure 1. (Top) STEM images of EVQ-218 showing particle uniformity with minimal grouping and relatively no agglomeration. Note the nearly equidistant spacing within the grouping of EVQ-218 NPs shown in the lower magnification images. (Bottom) STEM images of NIST NPs for comparison. Note the slight differences in the size and shape profiles of the NIST material that contains nonspherical and faceted particles.

ture[23] (additional process discussion is found in Supporting Information S3). In-depth characterization and speciation studies reveal that EVQ-218 is a new, unique AgNP that falls in line with NIST standard particles, yet bares its own unique features (i.e., a bare silver surface).

RESULTS

STEM Imaging of EVQ-218. *General Survey.* Figure 1 shows the scanning transmission electron microscopy (STEM) images of EVQ-218 at different magnifications, with comparative images of NIST nanoComposix material. EVQ-218 has a uniform sphere morphology and does not agglomerate upon deposition onto transmission electron microscopy (TEM) grids. Small self-assembled groupings are observed frequently, as exhibited in the lower magnification images in Figure 1 (top). The consistent grouping without agglomeration and near-equidistant particle spacing are indicative of the intrinsic particle surface-based stability in the absence of surfactants. Additional STEM images (bright field and dark field, DF) of EVQ-218 on carbon and SiO_2 TEM grids are presented in Supporting Information S5. Note the number of nonspherical particles in NIST images (Figure 1, bottom). Although most particles have a uniform size and shape, a portion contains facets and a hedral nature. Nonspherical particles such as these may have different stabilities and reactivities that should be considered in fate and application studies.

Dimensions and Size Distribution: DLS and TEM. Dynamic light scattering (DLS) measurements were obtained for EVQ-218 and NIST nanoComposix. In addition to mean particle size, it is important to report the statistical d(10), d(50), and d(90) values and provide greater insight into the particle size distribution. Statistical d(x) values (where x percent of NP is equal to or smaller than a given size) can be critical in applications where a too large/small NP is undesirable or toxic. Number density (# of NP per mL of solution) and specific surface area (active surface area per g of active NP) of NEAT suspensions were calculated based on these d values and are presented in Tables 1 and 2. DLS size profiles of both EVQ-218 and NIST nanoComposix agree with manufacturer specifications with similar narrow distribution results.

Table 1. Number Density and Specific Surface Area for EVQ-218

	particle size (diameter nm)	number density (NP/mL)	specific surface area (m^2/g)
d(10)	3.9	3.2×10^{13}	148.5
d(50)	8.0	3.5×10^{12}	71.1
d(90)	10.8	1.5×10^{12}	53.1

Table 2. Number Density and Specific Surface Area for nanoComposix NIST AgNP

	particle size (diameter nm)	number density (NP/mL)	specific surface area (m^2/g)
d(10)	8.5	3.0×10^{12}	67.5
d(50)	11.5	1.2×10^{12}	49.9
d(90)	13.7	7.0×10^{11}	41.6

EVQ-218 NP sizing using TEM imaging results agree with material specifications, with Gaussian distribution around 8−10 nm (Figure 2 below). NIST nanoComposix image-based sizing resulted in a similar Gaussian profile around 8−10 nm (Figure 3). Note the differences in sizing histograms, with EVQ-218 having a slightly tighter and more uniform profile.

Kinetic Dissolution Studies (KDS) of EVQ-218 and NIST nanoComposix. Upon exposure to moderately hard water (MHW, synthetic analogue), EVQ-218 solution immediately began to change color. A full color transition from yellow to peach/orange to red/pink to purple/blue occurred within 60 s. No such color change occurred in the NIST nanoComposix dilution in MHW. Upon exposure to 20X-AAP-supplemented dilution water (mineral-rich aquatic plant/algae growth media, synthetic analogue), both EVQ-218 and nanoComposix NIST solutions turned from yellow to grayish brown color. Within 48 h, EVQ-218 MHW and EVQ-218 20X-AAP exhibited complete loss of color and significant

https://doi.org/10.1021/acsomega.3c07745
ACS Omega 2024, 9, 7891−7903

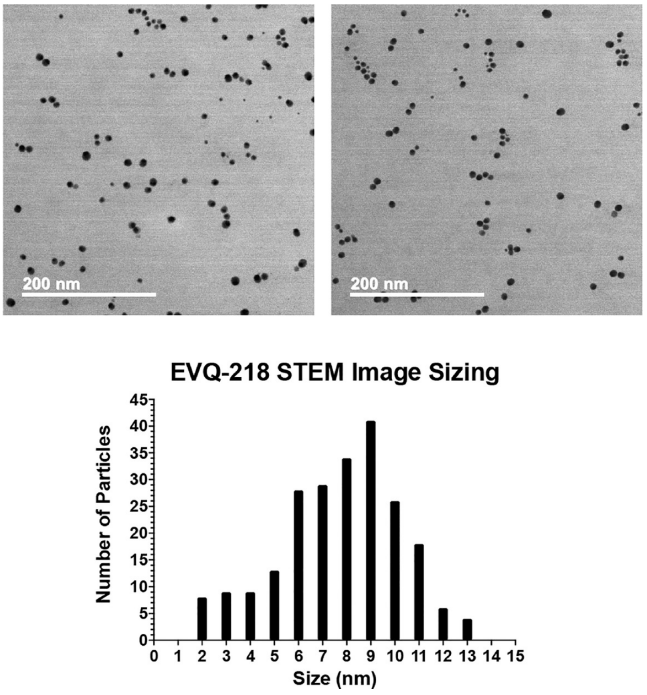

Figure 2. (Above) STEM images of EVQ-218 with resolution and particle counts suitable for particle sizing.[25] Note that the individual particle nature is maintained after deposition and evaporation. (Below) Particle size distribution obtained from STEM images (7.7 ± 2.5 nm).

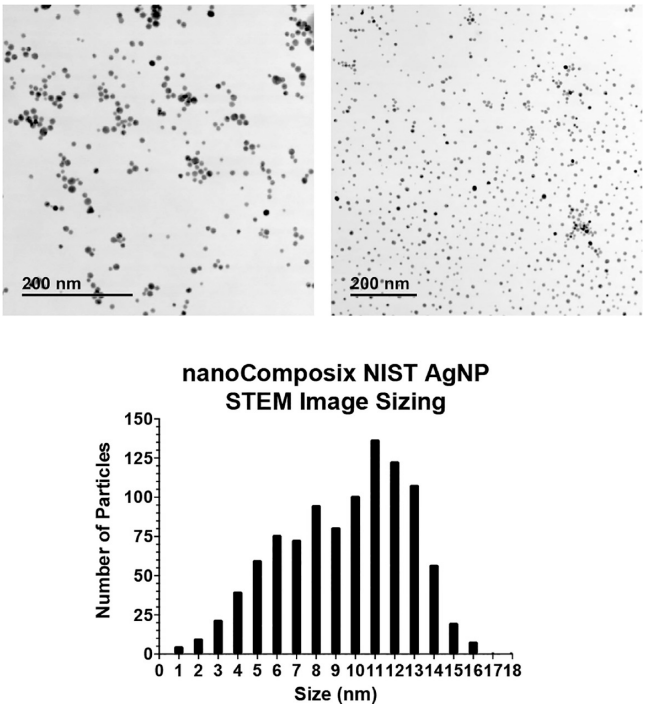

Figure 3. (Above) STEM images of NIST nanoComposix, with resolution and particle counts suitable for particle sizing.[25] Note that the individual particle nature is maintained after deposition and evaporation. (Below) Size distribution of NIST nanoComposix obtained from STEM images above (9.5 ± 3.2 nm) agrees with NIST-certified NP profile (10.3 ± 2.1 nm).

precipitation at the bottom of the flask. nanoComposix 20X-AAP samples exhibited similar fallout and loss of color; however, no precipitate or color change occurred with the MHW-exposed nanoComposix samples.

Turbidity measurements were obtained throughout the study but yielded similar uninformative results to those reported by Miller and Chappel.[26] Turbidity measurements were not markedly different for all samples except nanoComposix with MHW media, which had results below the limits of detection (BLOD).

Ion selective electrode (ISE) results (Supporting Information S7) reveal negligible ion content for all samples except EVQ-218 in MHW. All samples of EVQ-218 and nanoComposix exhibited significantly lower ISE results than particles presented by Miller and Chappell[26] Results for EVQ-218 in MHW do not correlate with the inductively coupled plasma-optical emission spectroscopy (ICP-OES) data presented above. As the ISE probe used in this study is silver/silver sulfide, it is possible that EVQ-218 particles may interact with the electrode surface and yield false positives. Further investigation of EVQ-218 versus silver ion is presented below.

KDS Ultracentrifugation. Preliminary validation was conducted to determine the conditions necessary to fully separate/isolate all solid NPs. Theoretically NP separation will occur with ultracentrifugation at 100,000 *g*-force for 1 h.[27] Several iterations were conducted at 100,000−150,000 *g*-force. EVQ-218 did not exhibit complete NP separation under these conditions. Centrifuge times were extended up to 18 h (150,000 *g*-force) with no increase in particle separation. NIST standard nanoComposix NPs were ultracentrifuged under identical conditions and exhibited complete separation within 6 h (Figure 4). Kinetic dissolution methods require frequent

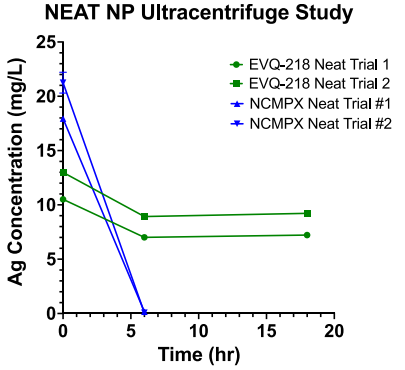

Figure 4. ICP-OES silver levels in EVQ-218 and nanoComposix (labeled NCMPX) after 1, 6, and 18 h ultracentrifuge trials at 150,000 *g* force.

silver analyses before and after centrifugation, so 6 h was established as maximum spin time realistic for this 48 h study. The significant levels of EVQ-218 after 18 h centrifugation required further investigation and are discussed further below.

After ultracentrifugation at 150,000 *g*-force for 18 h did not completely remove EVQ-218 from the suspension, high-resolution STEM imaging was conducted. The images below (Figure 5) show that significant levels of NPs remain in the suspension, largely in the 2 nm range. Most particle separation techniques rely on particles >4 nm; therefore, studies involving smaller particles require additional screening. Particle sizing was conducted[25] to further characterize the particles present after extended centrifugation (Figure 5).

KDS ICP-OES Results. Within 24 h, a significant amount of AgNPs reacted with supplemental minerals in the media. As

https://doi.org/10.1021/acsomega.3c07745
ACS Omega 2024, 9, 7891−7903

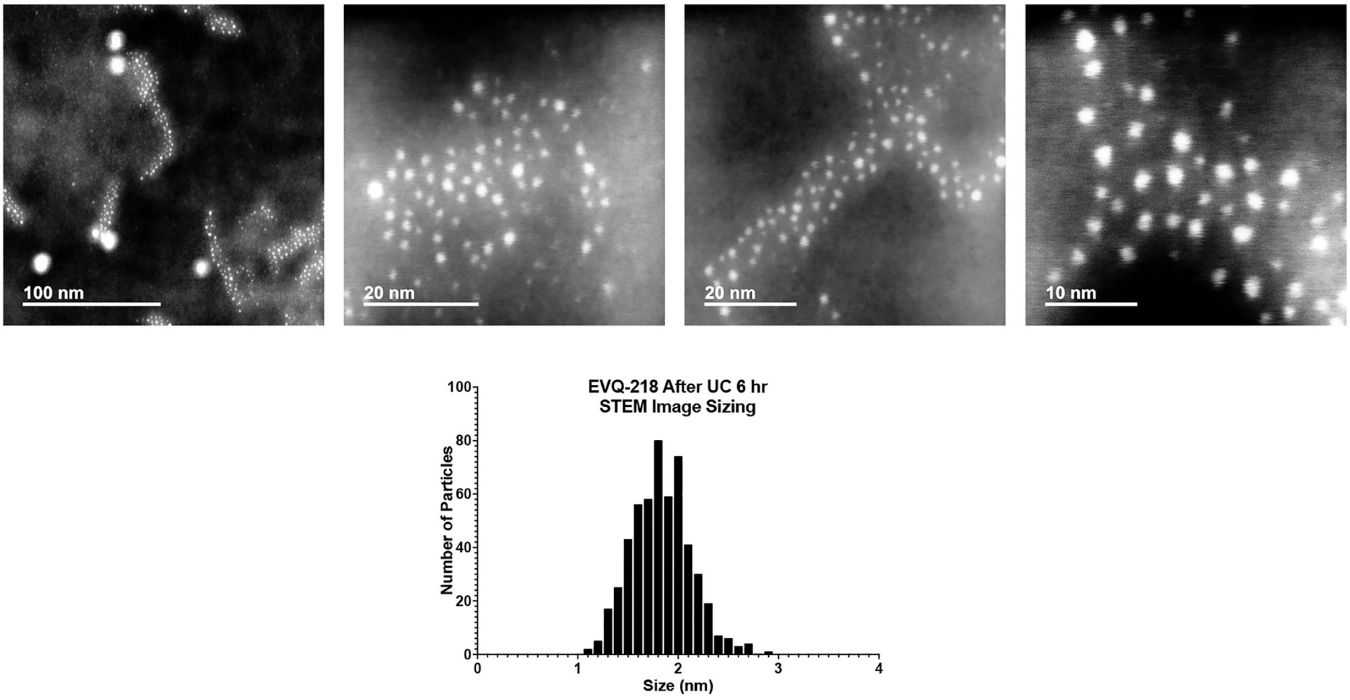

Figure 5. DF-STEM images of EVQ-218 after ultracentrifugation at 150,000 *g* force for 6 h. Note the significant amount of ∼2 nm particles present that self-assembled with equidistant spacing. STEM image particle size profile of EVQ-218 after ultracentrifugation at 150,000 *g* force for 6 h.

the NPs were coated, they seeded further precipitation with all samples, except nanoComposix in MHW, which did not exhibit fallout. As EVQ-218 interacted with these minerals, ultracentrifuge efficiencies were increased, particularly for the AAP samples. nanoComposix in MHW did not exhibit any particle fallout within 48 h. Samples were retained for several months after this study and did not exhibit fallout; however, the solution did exhibit color change toward red/orange to brown. Turbidity results were comparable for EVQ-218 in MHW/20X-AAP and nanoComposix in 20X-AAP; and BLOD for nanoComposix MHW correlates with rapid destabilization and precipitation of NPs.

ICP-OES results for all EVQ-218 and NIST nanoComposix in MHW and 20X-AAP media are presented in Figures 6 and 7. Silver levels before ultracentrifugation are in line with the visual precipitation trends. As EVQ-218 precipitates in MHW, ultracentrifuged silver levels approach 0 but did not reach the trace levels exhibited by EVQ-218 in 20X-AAP. The oxyanion species in 20X-AAP media can form bulk solids with the NP and other mineral cations. As a result, precipitation occurs more quickly in 20X-AAP media.

KDS Malvern DLS Particle Sizing Data. As both EVQ-218 and nanoComposix are both produced and obtained in DI water (never as a solid isolate), NEAT material size profiles were used to compare mineral-exposed particles over time.

DLS mean percent (percent intensity) size profiles shown in Figures 8 (EVQ-218) and 9 (nanoComposix) are reflective of actual particle counts rather than intensity. Larger particles result in more intense scattering that drowns out scattering from particles smaller than 20−40 nm. DLS data presented below fall in line with ICP-OES data with respect to particle size increase, precipitation, and dispersion stability. Note the lack of size increase for nanoComposix particles in MHW (Figure 9), which did not exhibit precipitation throughout the 48 h study.

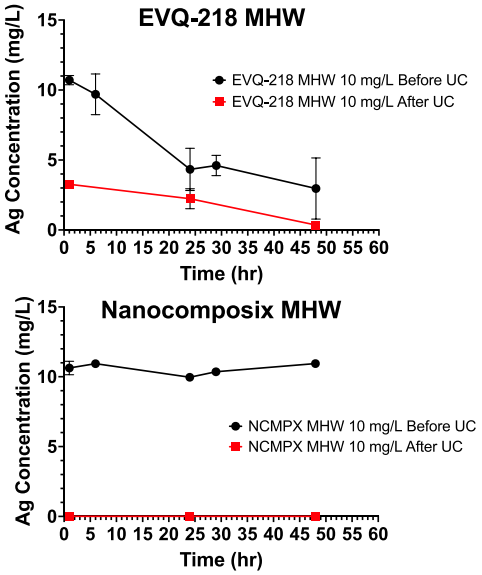

Figure 6. Silver ICP-OES results for EVQ-218 and NIST nanoComposix (labeled NCMPX) in MHW media at 10 mg/L; before (black) and after (red) 6 h ultracentrifugation.

Additional DLS data: In addition to the mean percent sizing data shown above, Miller and Chappell[26] presented DLS data reflecting aggregation modeling, as well as cumulant analysis Z-average/PDI (poly dispersity index). Equivalent data with respect to aggregation modeling are presented in Supporting Information S8 (Tables 1 and 2). Z-average/PDI-based data are presented in Supporting Information S9 (Tables 3 and 4).

Post KDS Follow-Up Studies: Imaging of AgNPs Post-KDS Mineral Exposure, Ag ion-treated EVQ-218, EELS. *Mineral-Exposed AgNPs STEM-EDS Analysis.* To gain further insight into possible behavior and reactivity differences between EVQ-218 and NIST, STEM imaging with EDS

https://doi.org/10.1021/acsomega.3c07745
ACS Omega 2024, 9, 7891−7903

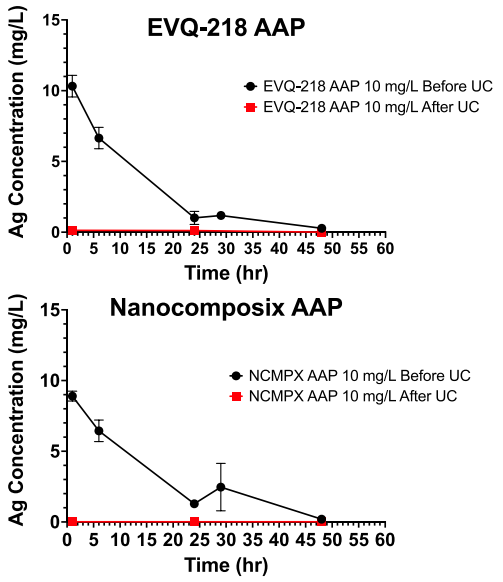

Figure 7. Silver ICP-OES results for EVQ-218 and NIST nanoComposix (labeled NCMPX) in 20X-AAP media at 10 mg/L; before (black) and after (red) 6 h ultracentrifugation.

mapping was conducted on all KDS precipitates and the NIST MHW dispersion. Figure 9 shows the STEM images of EVQ-218 and MHW. Note the spherical particle nature that is still obvious despite having fallen out of suspension. Chemical mapping from EDS spectra (Figure 10) reveals the $CaCO_3$ jacketed EVQ-218 particles and destabilized the suspension, inducing precipitation. Images of EVQ-218 exposed to AAP minerals (Figure 11) are quite different, with amorphous clusters of encapsulated and agglomerated particles. Figure 12 shows a wide variety of AAP minerals dispersed throughout the precipitate.

Imaging of NIST AgNP with MHW (Figure 13) shows an equivalent individual particle nature as untreated material. Trace signs of the $CaCO_3$ additive can be seen as a slight haze in some STEM images and in EDS mapping (Figure 14). Note that in Figure 13 (without capping agents or surfactants), some triangular/pyramidal AgNPs are present in the NIST material as chemical particle growth is difficult to control and size separation methods do not affect shape profiles. Where NIST material does not react with MHW, it behaves similar to EVQ-218 with AAP minerals. Figure 15 shows NIST AgNPs in amorphous clusters comparable to those in Figure 11. The citrate shell forms network solids with the sea of mineral ions, just as EVQ-218 does, and exhibits similar multielement EDS mapping (Figure 16).

Silver Ion Exposed EVQ-218 Images. Early studies of EVQ-218 with respect to possible ion content included exposing EVQ-218 to silver ions. Separation techniques employed to quantify ionic content/emission would require selectivity of ions vs NPs. STEM imaging of EVQ-218 exposed to silver ion (Figure 17) provide notable evidence that EVQ-218 does not emit ions.

The images above (Figure 17) show that upon exposure to silver ion, EVQ-218 is readily coated with a different silver structure. If EVQ-218 did emit ions, then there would be a continual emission and replating of silver on the surface of every particle. All of the images of EVQ-218 presented in the sections above were collected at least 12 months after manufacture. If EVQ-218 emitted ions or had ions present in solution, the uniformity presented above would not exist. Retention samples of EVQ-218 dating back to 2007 were maintained and revisited since their production. Below (Figure 18) are images of EVQ-218 from 2007 that were included in a study from 2020. The robust stability of EVQ-218 is unlike any traditional AgNPs to date and makes it a promising additive for long-term material applications not possible with current emissive species.

STEM-EELS Analyses. Several comparative differences are observed after in-depth STEM imaging with EELS mapping. Although similar in size, the surface chemistry of the two particles is different, most likely due to the contraction of surface atoms created by the high-energy ATTOSTAT process. EVQ-218 particles therefore exhibit different surface chemistry, kinetics, antimicrobial activity, and toxicity. Figures 19 and 20 reveal that there is a lack of oxygen/oxide layer around the EVQ-218 particles; that is obvious in the nanoComposix EELS mapping in Figures 21 and 22. Overall, EVQ-218 NPs exhibit a more uniform spherical nature, with less faceting than the NIST standard. This surface morphology is conducive to surfactant-free stability as geometric effects between EVQ-218 NPs occur, creating a self-stabilizing dispersion. Agglomeration is reduced and mitigates the need for capping agents commonly used in nanomaterial production.

DISCUSSION

Qualitative TEM imaging of EVQ-218 (Figure 1) shows the particle size and morphology comparable to NIST standard AgNPs. Sizing data from TEM image analysis (Figures 2 and 3) and DLS (Tables 1 and 2) further establishes the particle profile similarities between EVQ-218 and NIST AgNPs. Both species are comprised of highly uniform ∼10 nm spherical AgNP, which could be mistaken for equivalent additive ingredients without further investigation of particle stability and surface chemistry. NIST nanoComposix bare/citrate AgNPs are dispersed in 2 mM citrate buffer solution that serves both as a size control/capping reagent during synthesis and a final product stabilization/surfactant species. While NIST AgNPs contain ∼10x molar ratio citrate:NP, EVQ-218 contains only AgNPs in 18 MΩ H_2O, without added stabilizers/surfactants. Despite the large excess of citrate stabilizer in NIST AgNP, this material only has a shelf life in the range of weeks and requires refrigeration. In stark contrast, EVQ-218 has a shelf life of months to years without stabilizing chemistry or refrigeration. These enhanced properties, along with a scalable single step method of manufacture, make EVQ-218 an intriguing rival to the numerous commercial silver species on the market. Understanding the differences between these suspensions (and their corresponding chemistries) is key to understanding AgNP interactions in other chemical environments and applications.

Investigating the effects of mineral exposure to AgNPs sheds light on the potential environmental fate as well as preliminary formulation/compatibility information. KDS data revealed that EVQ-218 is rapidly destabilized in mineral-rich and hardened aquatic environments. Similar high mineral destabilization occurred with NIST AgNPs upon AAP exposure but did not occur with MHW exposure. The lack of reactivity with MHW is indicative of the outer nature of nanoComposix NPs, which do not have a truly bare surface, as advertised. The citrate shell on NIST AgNPs has carboxyl groups like $CaCO_3$ that prevent surface adhesion. High mineral AAP media contain a variety of metal cations and oxyanion species that facilitate formation of

https://doi.org/10.1021/acsomega.3c07745
ACS Omega 2024, 9, 7891−7903

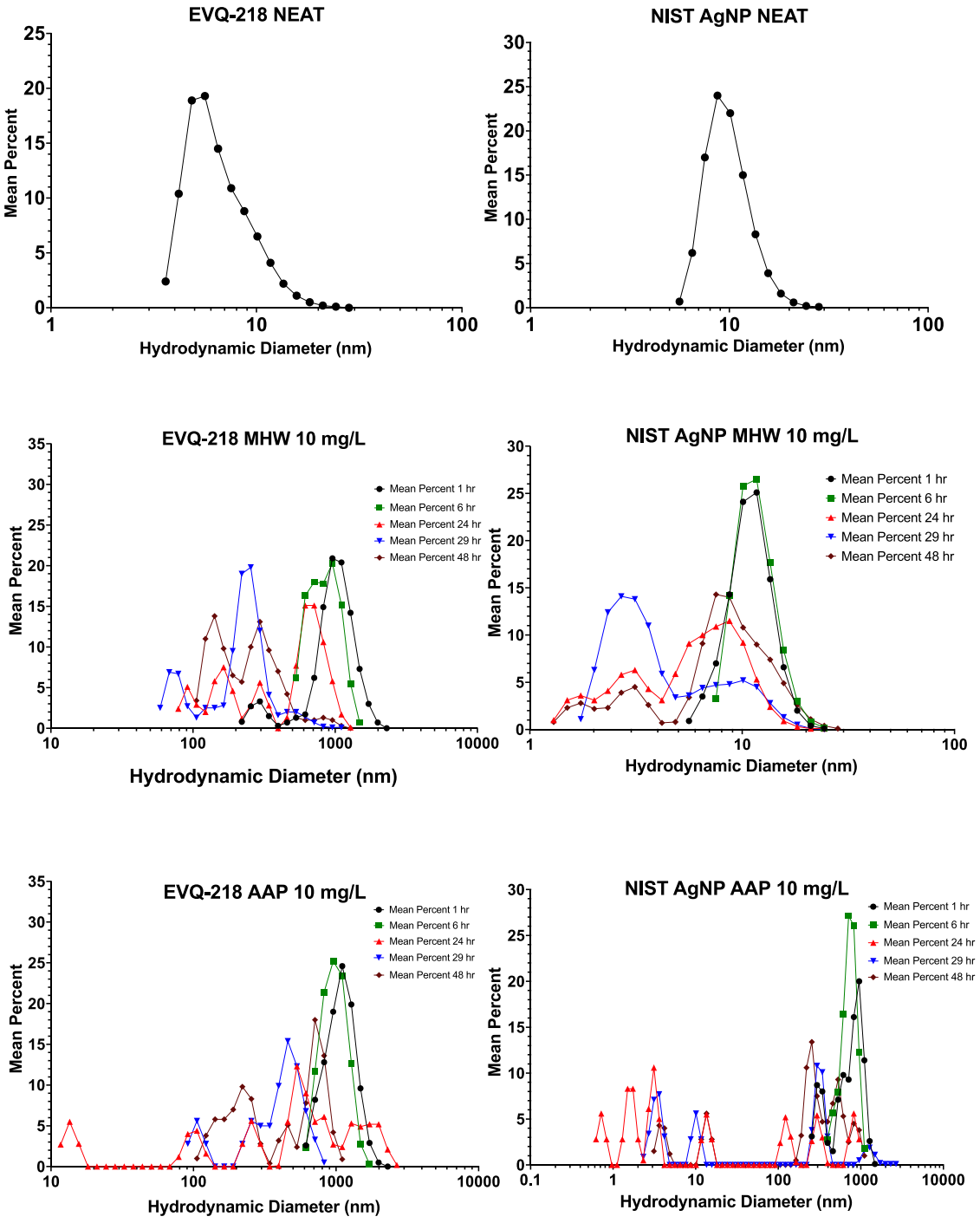

Figure 8. DLS particle size data for NEAT EVQ-218 (top left), NEAT NIST AgNP (top right), EVQ-218 with MHW (middle left), NIST AgNP with MHW (middle right), EVQ-218 with AAP (bottom left), and NIST AgNP with AAP (bottom right) media environments. Note the increase in particle size over time for all NP exposures except for NIST AgNP with MHW.

network solids. Ions quickly interact with the citrate NIST shell and the bare silver surface of EVQ-218, inducing precipitation and agglomeration. STEM-EDS analyses (Figures 9–16) of exposed EVQ-218 and NIST AgNPs verify this precipitation effect, with significant overlap of Ag and relevant mineral elemental maps. These results emphasize the need to screen all candidate AgNP species against various formulary ingredients during early developmental studies. Identification of incompatible additives allows for more efficient development of functional enhanced products.

Results from KDS studies satisfy short-term stability questions, but they do not address potential long-term emissive effects. Over time, typical AgNPs emit potentially toxic silver ions, and analytical methods may not have limits of detection suitable for ion quantification. Developmental studies of EVQ-218 yielded surprising qualitative evidence of its nonemissive nature. Samples of EVQ-218 doped with $AgNO_3$ prior to ion selectivity studies provide STEM image validation of how readily exposure to silver ions causes particle deformation (Figure 17). Emissive nature would be evident, and samples of EVQ-218 would not exhibit particle stability lasting months to

https://doi.org/10.1021/acsomega.3c07745
ACS Omega 2024, 9, 7891−7903

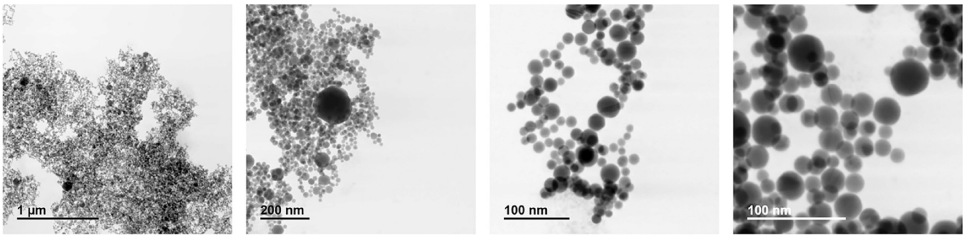

Figure 9. STEM images of precipitate from EVQ-218 exposed to MHW. Note that the spherical nature is still apparent even after agglomeration and precipitation.

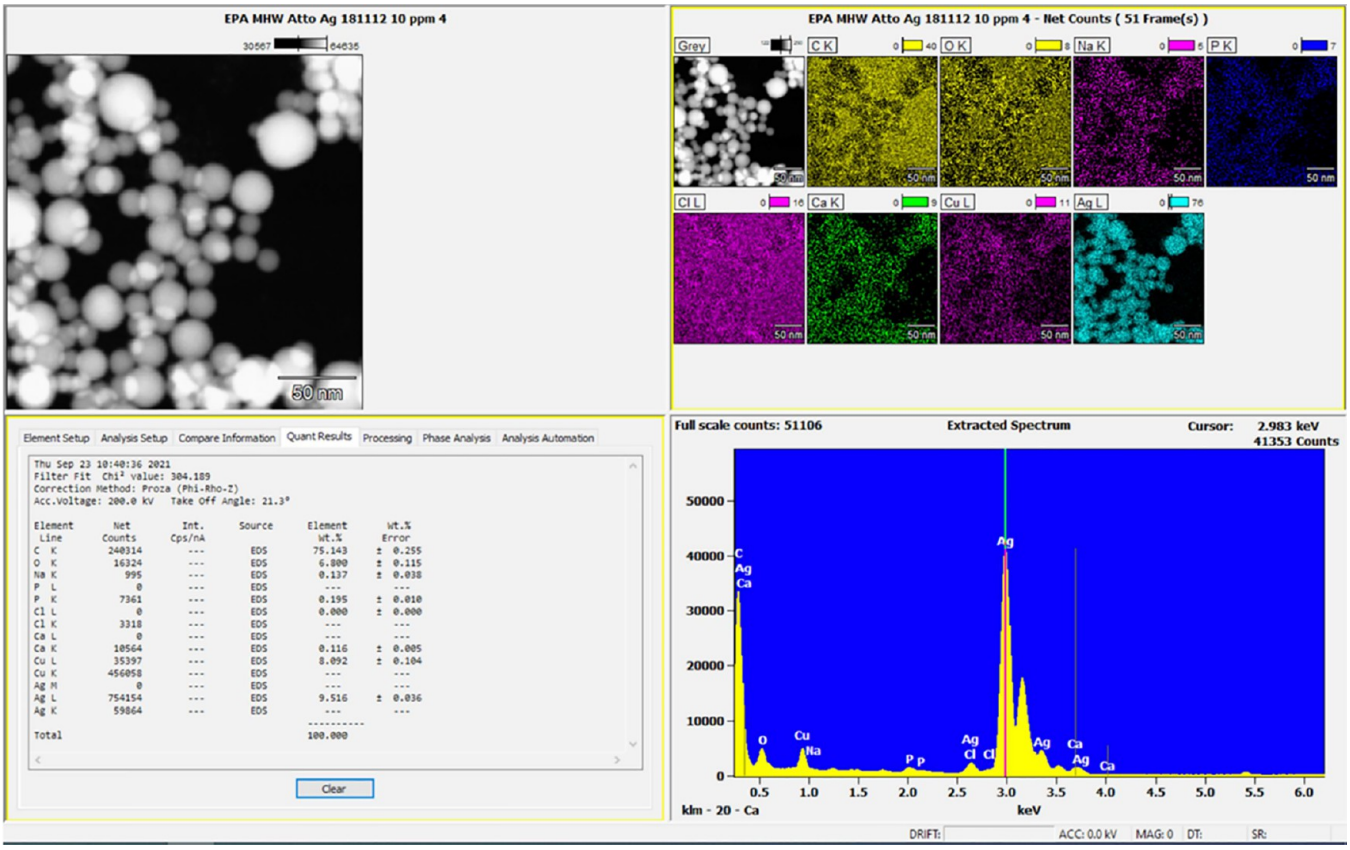

Figure 10. EDS mapping of mineral-exposed EVQ-218 with Ag signals that distinctly overlap with the reference STEM image. Note the distinct Ca, C, and O overlap that was not present in NEAT EVQ-218.

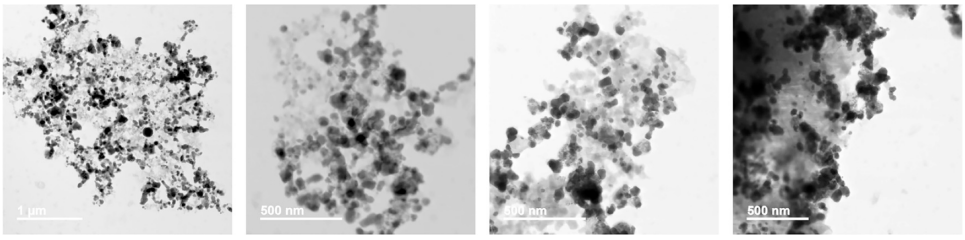

Figure 11. STEM images of precipitate from EVQ-218 exposed to 20X-AAP (higher magnification). Note that the spherical nature is less apparent after agglomeration/cocrystallization.

years. This is of particular interest to textile and medical device manufacturers as current AgNP-enhanced products have short-term use profiles due to silver leaching over time. Many of these products also use excess AgNPs that adds to the ongoing environmental risk discussion. The nonemissive nature of EVQ-218 makes it an attractive candidate for these applications and has led to a queue of product development studies.

High-resolution STEM-EELS analysis reveals the distinct difference in surface chemistry between EVQ-218 and NIST. It also sheds light on the long-term, nonemissive stability of EVQ-218. The bare Ag surface of EVQ-218 is unlike any NIST AgNP species, providing intrinsic stability and preventing ion

https://doi.org/10.1021/acsomega.3c07745
ACS Omega 2024, 9, 7891−7903

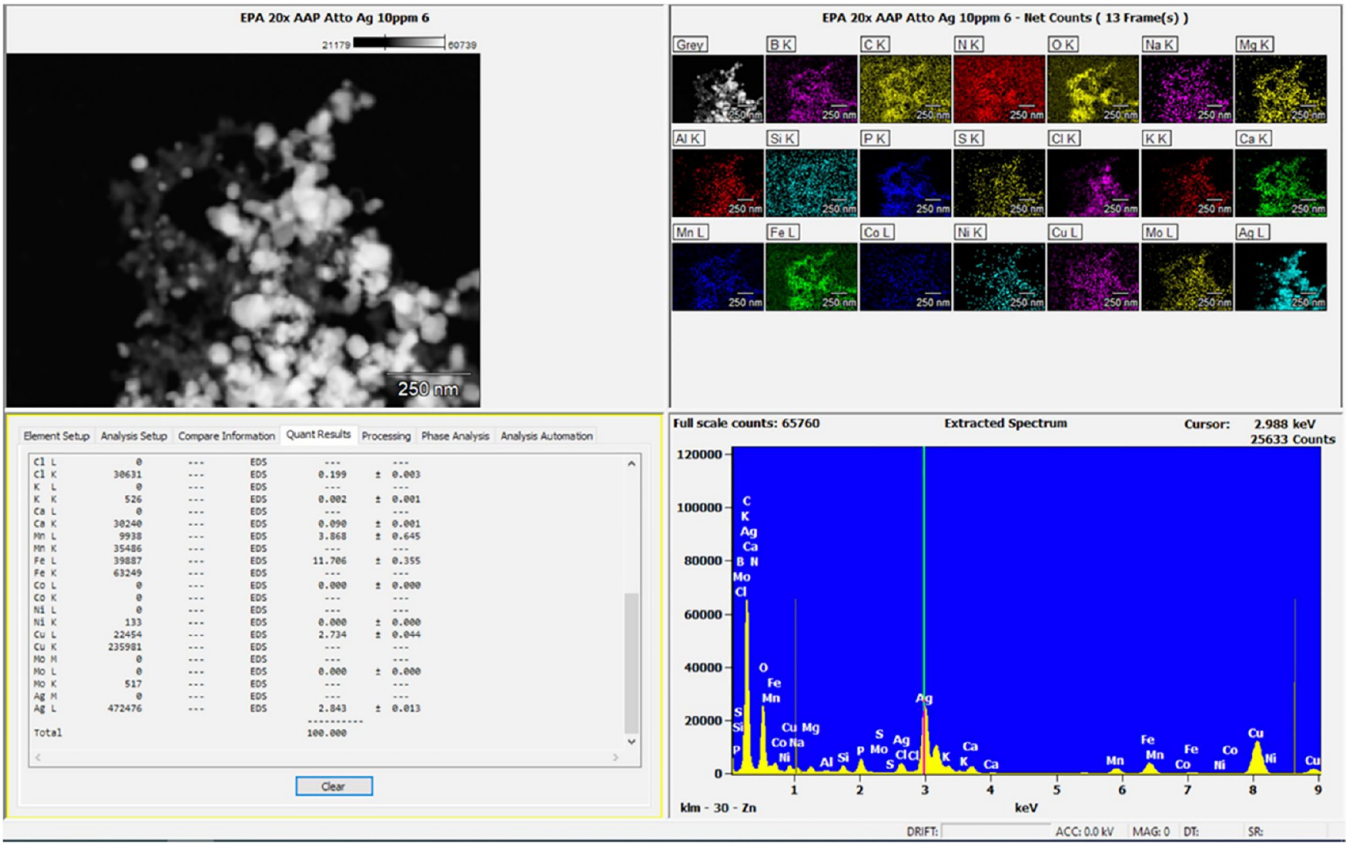

Figure 12. EDS mapping of mineral-exposed EVQ-218 with Ag signals that distinctly overlap with the reference STEM image. Note the distinct overlap of several mineral elements that were not present in NEAT EVQ-218.

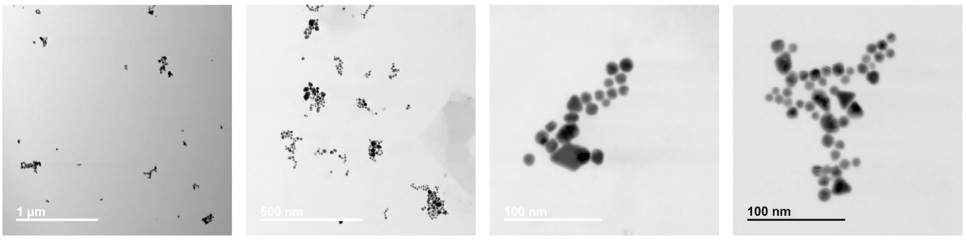

Figure 13. STEM images of nanoComposix NIST AgNPs exposed to MHW. Note the uniform particle nature even after MHW exposure, which agrees with the lack of agglomeration/precipitation.

emission. It is noteworthy that the high-energy EVQ-218 manufacturing process facilitates the generation of particles with a greater number of atoms per surface area, with shorter bond lengths. The multilaser process harnesses energy on par with diamond formation and generates particles with similar enhanced stability. From the BOLS model of chemistry, this increases the stability of the particle to the point of requiring an extreme acid with a high oxygen reduction potential (ORP) like aqua regia to disassociate the particles into ions. Also, the higher atomic density surface of the EVQ-218 particles would have greater interaction potential with surrounding chemistry such as sulfur, chloride, phosphorus, sodium, and potassium. Complementary techniques like STEM-EDS and EELS can provide greater insight into stability and reactivity of engineered NPs and aid application research and development.

The KDS and characterization studies conducted with EVQ-218 support the importance of screening engineered nanomaterials as thoroughly as possible. Not all particles are suitable for established methods such as those employed by Miller and Chappell,[26] and additional testing may be necessary. For example, EVQ-218 is not readily removed from suspensions using conventional ultracentrifugation techniques. Also, at the trace levels investigated in this study, any emitted ions should be precipitated upon exposure to chloride or carbonate ions. ICP-OES and ISE measurements presented above could be interpreted as evidence of ionic silver; however, stoichiometry and other data from EVQ-218 studies do not support ionic silver presence. A multifaceted analytical approach is critical during NP-enhanced product development and will facilitate the launch of functional, reliable, and safe products.

CONCLUSIONS

Extensive characterization studies show that EVQ-218 is a new form of AgNP, made possible by a patented high-energy manufacturing process that requires only laser (light) energy, 18 MΩ water, and pure silver metal. Ablation energy during EVQ-218 production achieves temperatures and pressures on par with that of diamond formation and results in a similar

https://doi.org/10.1021/acsomega.3c07745
ACS Omega 2024, 9, 7891−7903

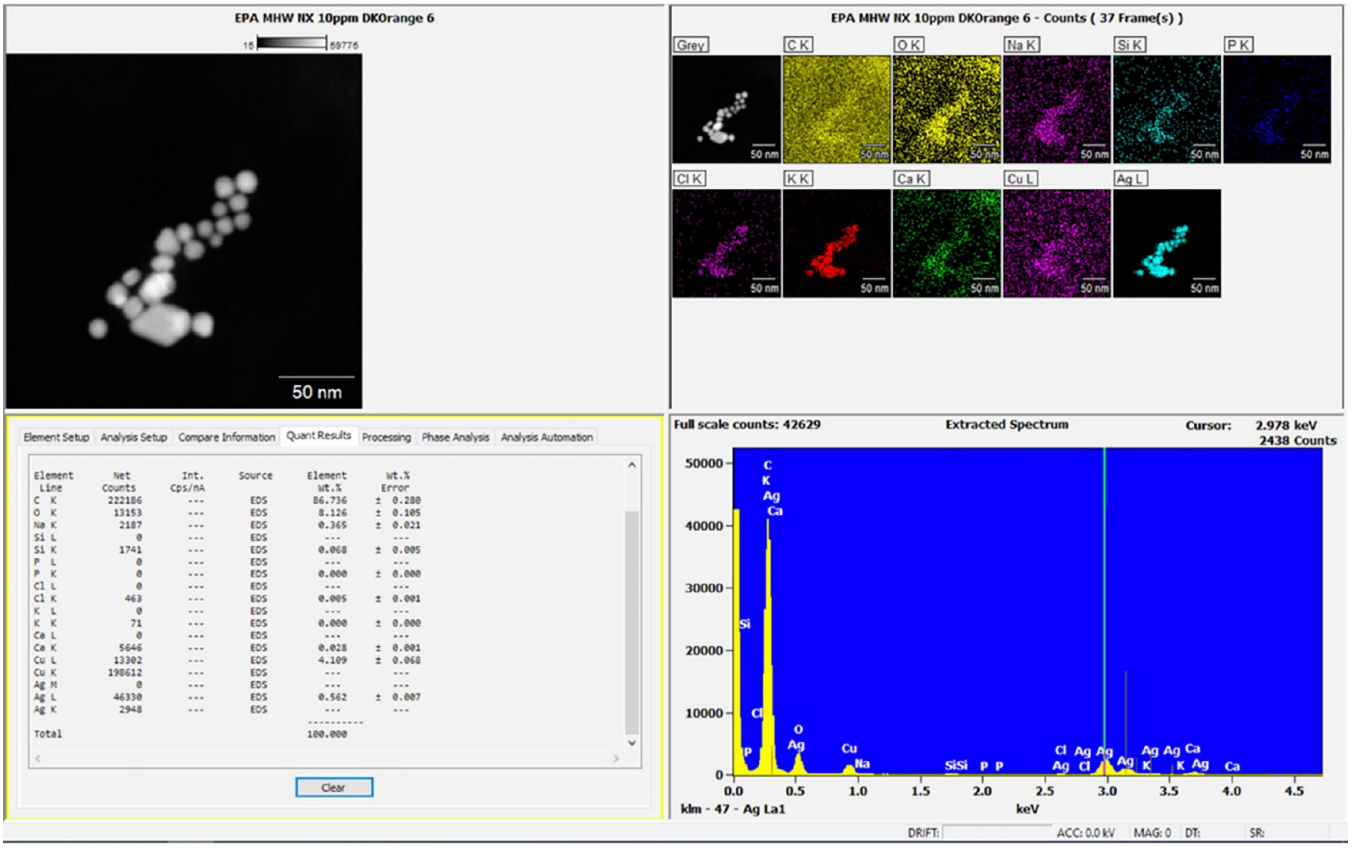

Figure 14. EDS mapping of mineral-exposed nanoComposix NIST AgNPs with Ag signals that distinctly overlap with the reference STEM image.

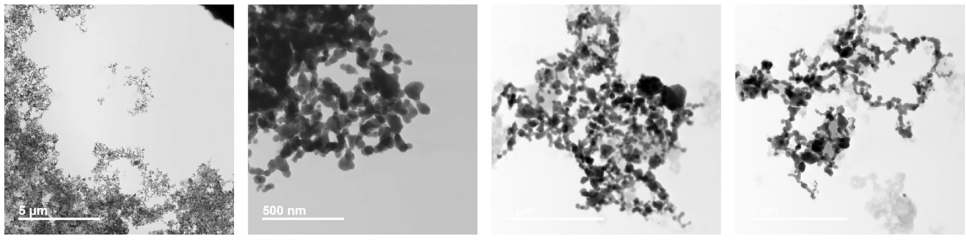

Figure 15. STEM images of precipitate from nanoComposix NIST AgNPs exposed to 20X-AAP (higher magnification). Note the spherical nature is less apparent after agglomeration/cocrystallization.

robust, nonemissive surface structure. Side-by-side comparison with NIST standard AgNPs reveals that EVQ-218 has equivalent spherical particle uniformity with respect to size profile and morphology. Unlike the citrate and polymer coated NIST standard AgNPs, EVQ-218 particles have true "bare" silver surface chemistry with greater group stability that mitigates the need for added stabilizers. The single-step ATTOSTAT method produces particles with very narrow size distribution that mitigates the need for tedious size fractionation processes required for NIST standards, and it is scalable to meet industrial demand. As EVQ-218 does not emit ions, it has far less risk potential and makes longer-term materials application possible. These qualities make EVQ-218 a cleaner standalone material than current NIST standard AgNPs and an intriguing candidate for a variety of applications. The unique and pure nature of EVQ-218 is a direct result of the high-energy ATTOSTAT method and may constitute the new gold standard for silver nanomaterials.

EXPERIMENTAL SECTION

Materials. EVQ-218 was produced directly into 18 MΩ water according to patented methods.[23] Silver target material (99.999% silver rod) was obtained from ESPI Metals. NP yield is nearly 100%, with negligible particle adhesion to the fluid tubing. Batches of EVQ-218 were analyzed via ICP-OES, STEM, and DLS prior to KDSs. NIST silver NPs (nanoComposix: 20 ppm of NanoXact bare/citrate in 2 mM citrate, AGCN10: Lot RRR0028) were screened alongside EVQ-218 in all studies as a nonionic/nonemissive comparative.

DLS-Based Particle Sizing. NEAT samples of EVQ-218 and NIST nanoComposix were screened for initial size profile using a Malvern Zetasizer NanoSeries (in line with NIST-NCL PCC-1) instrument.[24] As DLS measures the hydrodynamic diameter, direct comparison using STEM is needed to ensure accurate particle dimensions.

Image-Based Particle Sizing and XRD. STEM images were acquired according to NIST-NCL PCC-7.[25] Samples (of EVQ-218 and nanoComposix NIST) were deposited onto

https://doi.org/10.1021/acsomega.3c07745
ACS Omega 2024, 9, 7891−7903

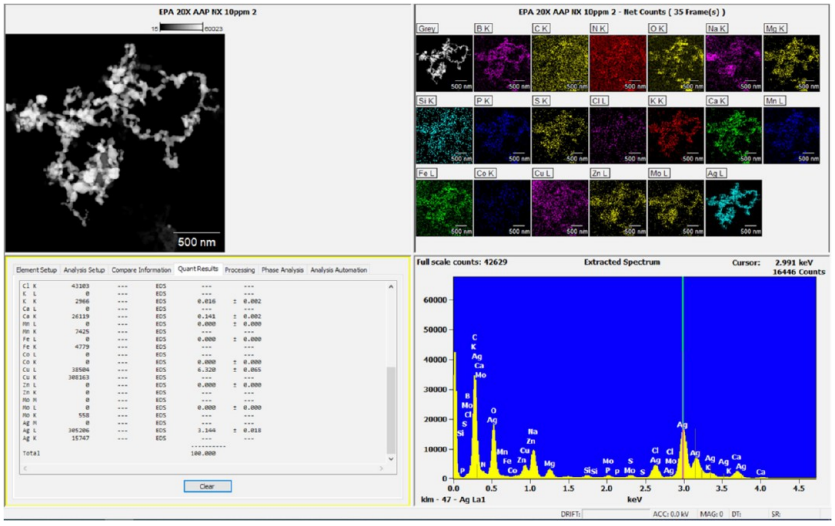

Figure 16. EDS mapping of mineral-exposed nanoComposix NIST AgNPs with Ag signals that distinctly overlap with the reference STEM image. Note the distinct overlap of several mineral elements that are not present in NEAT nanoComposix NIST AgNPs.

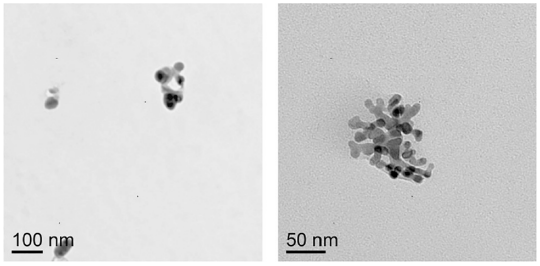

Figure 17. EVQ-218 exposed to $AgNO_3$ shows altered morphology and metallic density.

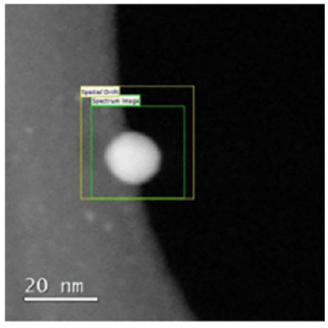

Figure 19. Single EVQ-218 NP area of interest with the spatial drift area defined (yellow square) and the spectrum image defined (green square).

PELCO carbon type B Grids (300 mesh, Ted Pella Inc.) or PELCO silicon dioxide (SiO_2) support films (40 nm, 50 × 50 μm) and imaged using a JEOL JEM-2800 microscope. Sizing methods were validated using NIST standard polystyrene (Thermo Scientific Nanosphere 3020A, 20 nm, lot number 211467. Data in Supporting Information S10). During particle imaging, X-ray Diffraction (XRD) patterns were collected for EVQ-218 and NIST particles for qualitative structural comparison. Diffraction patterns are presented in S11.

KDS Method. Ion emission from metallic NPs is a main area of concern with the biologic and environmental fate of engineered nanomaterials. An Army corps of engineers' study[26] outlines key data points to be collected when screening nanoscale active ingredients. These studies involve kinetic measurements of ionic and particulate content in a variety of natural systems (i.e., mineral-rich water or salt water to mimic natural environments). Silver analyses were conducted using ICP-OES and ISE. DLS measurements were carried out as well as ultracentrifugation to quantify particles vs ions over time. Both EVQ-218 and NIST nanoComposix particles were investigated, giving a side-by-side comparison of NEAT, in synthetic MHW and AAP media. Both types of particles were investigated at 10 mg/L AgNPs in both types of media.

NP solutions were added to synthetic MHW (80 mg/L $CaCO_3$) to achieve a final concentration of 10 mg/L. NP dilutions for 20X-AAP media were prepared by the addition of mineral stock solutions to dilution water to achieve 10 mg/L. All dilutions were performed within OECD aquatic media guidelines. NP solutions were prepared in triplicate, with sampling intervals at 1, 6, 24, 29, and 48 h. Suspension stability was monitored using ICP-OES silver analyses, silver ISE

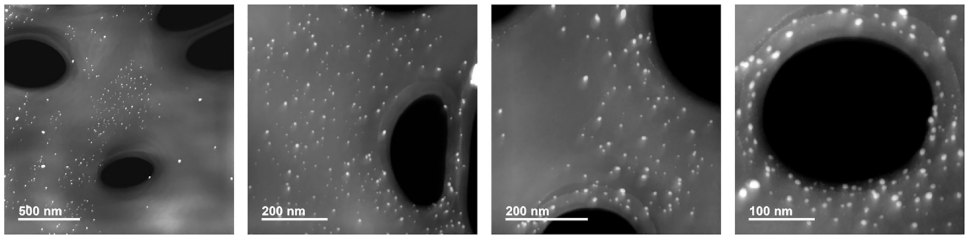

Figure 18. EVQ-218 produced in 2007, imaged on lacey carbon in 2020. Note the uniform silver density within the particles, indicative of a material that has not been exposed to ionic silver.

https://doi.org/10.1021/acsomega.3c07745
ACS Omega 2024, 9, 7891−7903

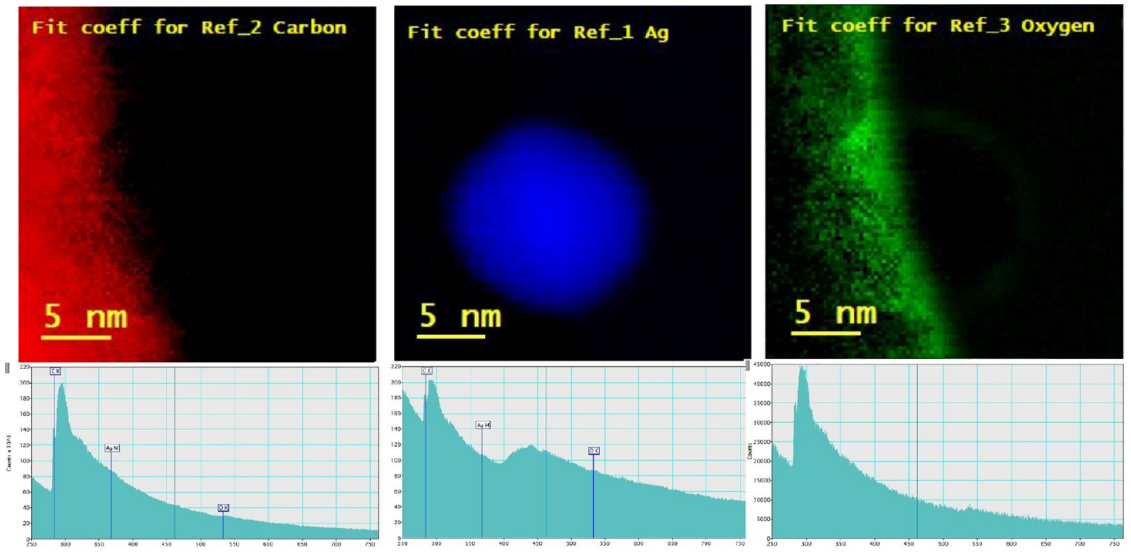

Figure 20. EVQ-218 EELS spectrum image map, low loss dark reference corrected with the spectrum of area of interest. Color-coded elemental maps of carbon (red), silver (blue), and oxygen(green) show that EVQ-218 has no outer oxygen content and is indeed a "bare" particle.

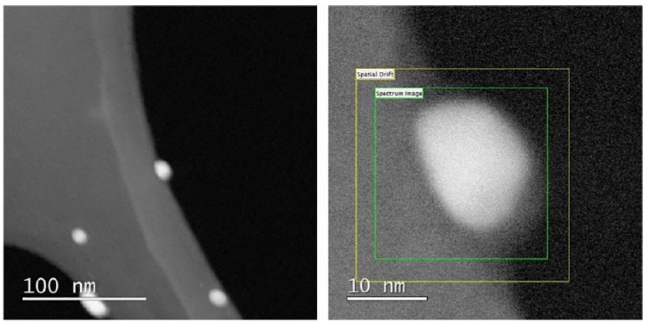

Figure 21. (Left): NIST nanoComposix on lacey carbon filament. (Right): Single particle area of interest (center particle in the image on the left) with the spatial drift area defined (yellow square) and the spectrum image defined (green square).

measurement, turbidity, and DLS particle sizing. As both nanomaterials are prepared/sold as aqueous suspensions in DI water, a 48 h DI water study was not applicable. Upon study completion, retention samples of each mixture were obtained for STEM imaging with EDS chemical mapping.

KDS ICP Method. NEAT samples of EVQ-218 and NIST nanoComposix were analyzed for the initial Ag content. Aliquots of mineralized solutions (5 mL) were taken from each flask at 1, 6, 24, 29, and 48 h. At 1, 24, and 48 h, a 6.5 mL aliquot was taken from each flask for ultracentrifugation, and ICP-OES measurements were made from each 5 mL natant sample. All ICP analyses were conducted using a PerkinElmer Optima 8000 spectrometer with an S10 autosampler. Samples were digested using a high ORP aqua regia method with sonication at 40 °C for 40 min and then diluted to 50.0 mL.

KDS DLS Method. Samples were measured using DLS, with aliquots (1−2 mL) taken from each flask at 1, 6, 24, 29,

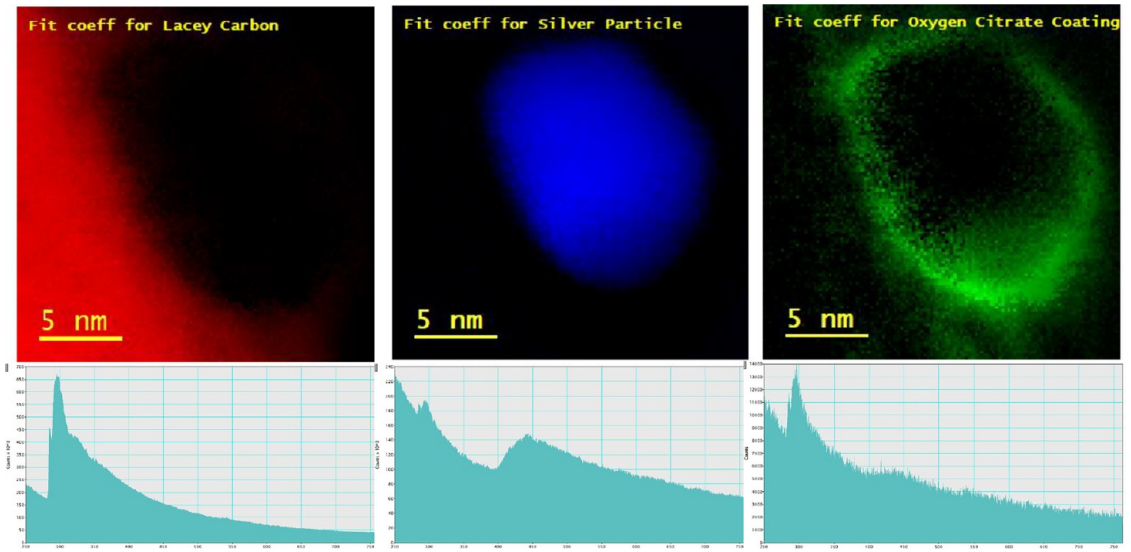

Figure 22. NIST nanoComposix "bare" EELS spectrum image map, low loss dark reference corrected with the spectrum of area of interest. Color-coded elemental maps of carbon (red), silver (blue), and oxygen (green) show that NIST particles have significant outer oxygen content and are not "bare" particles, as advertised.

https://doi.org/10.1021/acsomega.3c07745
ACS Omega 2024, 9, 7891−7903

and 48 h. Kinetic DLS measurements reveal how the size changes upon exposure to minerals and ions.

KDS ISE Method. NEAT samples of EVQ-218 and NIST nanoComposix were analyzed for initial ionic profile at all KDS time points. Silver ISE measurements were obtained by using an oakton silver/sulfide combination ISE. The surface of the electrode was reconditioned before each analysis, along with recalibration at 0, 1, 5, and 10 mg/L.

KDS Ultracentrifugation. NEAT samples of EVQ-218 and NIST nanoComposix were ultracentrifuged at 150,000-force for up to 18 h. Natant samples were analyzed via ICP-OES to determine the residual NP/ion content. When trialing this method, EVQ-218 did not fully sediment in 18 h, and kinetic measurements must be done daily. To obtain sufficient data density, 6 h cycles at 150,000 *g* force were performed on 1, 24, and 48 h samples. ICP-OES values were compared before and after ultracentrifugation to monitor the ion/NP ratios.

STEM-EELS Method. To obtain a better understanding of the individual particle characteristics, an electron microscope with an electron energy loss spectrometer was employed to image the elements and their states. Both EVQ-218 and NIST NPs were deposited on 300 mesh copper EM grids with lacey type B carbon filament that allowed single particle analyses. Images and EELS spectra were obtained using a JEOL ARM200F STEM system with an EELS spectrometer. High-resolution chemical mapping and surface chemistry information were obtained through elemental electron decay identification and Chi Square fits of the maps to ensure data confidence. Post processing was performed on GATAN EELS Analysis software.

■ ASSOCIATED CONTENT

Supporting Information

The Supporting Information is available free of charge at https://pubs.acs.org/doi/10.1021/acsomega.3c07745.

> Rationale behind patented laser ablation process: protoparticle manipulation during liquid-phase laser ablation; STEM imaging of EVQ-218: general survey of uniformity and grouping; ISE results from KDS; additional DLS data from KDS; TEM-based particle sizing method validation using NIST standard polystyrene; XRD pattern of EVQ-218 and NIST nanoComposix; and STEM-EDS analysis of EVQ-218 and NIST AgNPs exposed to MHW and AAP (PDF)

■ AUTHOR INFORMATION

Corresponding Author

Bretni S. Kennon − *EVŌQ Nano, Salt Lake City, Utah 84119, United States;* orcid.org/0009-0005-8646-4379; Email: bretnikennon@evoqnano.com

Author

William H. Niedermeyer − *EVŌQ Nano, Salt Lake City, Utah 84119, United States*

Complete contact information is available at: https://pubs.acs.org/10.1021/acsomega.3c07745

Notes

The authors declare no competing financial interest.

■ ACKNOWLEDGMENTS

Research presented in this article was directly funded by EVŌQ Nano, SLC, UT. The manuscript was written through contributions of all authors. All authors have given approval to the final version of the manuscript. We thank the University of Utah Nanofab Surface Analysis Lab* and the Arizona State University John M. Cowley Center for High-Resolution Electron Microscopy for allowing us access to their instrumentation. Special thanks to Brian van Devener and Manuel Roldan Gutierrez for their training, and expertise throughout our studies. *This work made use of University of Utah USTAR shared facilities supported in part by the MRSEC Program of the NSF under award No. DMR-1121252.

■ ABBREVIATIONS

EELS, Electron Energy Loss Spectroscopy; NCL, Nanotechnology Characterization Laboratory; PCC, Particle Characterization Collection; NIST, National Institute of Standards and Technology

■ REFERENCES

(1) Alexander, J. W. History of the Medical Use of Silver. *Surgical Infections* **2009**, *10* (3), 289.

(2) Medici, S.; Peana, M.; Nurchi, V. M.; Zoroddu, M. A. Medical Uses of Silver- History, Myths, and Scientific Evidence. *J. Med. Chem.* **2019**, *62*, 5923−5943.

(3) Sim, W.; Barnard, R. T.; Blaskovich, M. A. T.; Ziora, Z. M. Antimicrobial Silver in Medicinal and Consumer Applications: A Patent Review of the Past Decade (2007−2017). *Antibiotics* **2018**, *7*, 93.

(4) Kumar, A.; Goia, D. V. Comparative Analysis of Commercial Colloidal Silver Products. *Int. J. Nanomed.* **2020**, *15*, 10425−10434.

(5) Pourzahedi, L.; Vance, M.; Eckelman, M. J. Life Cycle Assessment and Release Studies for 15 Nanosilver-Enabled Consumer Products: Investigating Hotspots and Patterns of Contribution. *Environ. Sci. Technol.* **2017**, *51*, 7148−7158.

(6) Zhang, N.; Xiong, G.; Liu, Z. Toxicity of metal-based nanoparticles: Challenges in the nano era. *Front. Bioeng. Biotechnol.* **2022**, *10*, No. 1001572.

(7) Ferdous, Z.; Nemmar, A. Health Impact of Silver Nanoparticles: A Review of the Biodistribution and Toxicity Following Various Routes of Exposure. *International Journal of Molecular Sciences* **2020**, *21*, 2375.

(8) Stabryla, L. M.; Johnston, K. A.; Millstone, J. E.; Gilbertson, L. M. Emerging investigator series: it's not all about the ion: support for particle-specific contributions to silver nanoparticle antimicrobial activity Environ. *Sci. Nano* **2018**, *5*, 2047−2068.

(9) Kedziora, A.; Speruda, M.; Krzyzewska, E.; Rybka, J.; Bugla-Ploskonska, G. Similarities and Differences between silver ions and silver in nanoforms as antibacterial agents. *Int. J. Mol. Sci.* **2018**, *19*, 444.

(10) Slavin, Y. N.; Asnis, J.; Häfeli, U. O.; Bach, H. Metal nanoparticles: understanding the mechanisms behind antibacterial activity. *J. Nanobiotechnol.* **2017**, *15*, 65.

(11) Liao, C.; Li, Y.; Tjong, S. C. Bactericidal and Cytotoxic Properties of Silver Nanoparticles. *Int. J. Mol. Sci.* **2019**, *20*, 449.

(12) Gupta, V.; Mohapatra, S.; Mishra, H.; Farooq, U.; Kumar, K.; Ansari, M. J.; Aldawsari, M. F.; Alalaiwe, A. S.; Mirza, M. A.; Iqbal, Z. Nanotechnology in Cosmetics and Cosmeceuticals-A Review of Latest advancements. *Gels* **2022**, *8*, 173.

(13) Barrena, R.; Casals, E.; Colón, J.; Font, X.; Sánchez, A.; Puntes, V. Evaluation of the ecotoxicity of model nanoparticles. *Chemosphere* **2009**, *75*, 850−857.

(14) Gilga, A. R.; Skoglund, S.; Wallinder, I. O.; Fadeel, B.; Karisson, H. L. Size-dependent cytotoxicity of silver nanoparticles in human

lung cells: the role of cellular uptake, agglomeration, and Ag release. *Part. Fibre Toxicol.* **2014**, *11*, 11.
(15) Zhang, Z.; Shen, W.; Xue, J.; Liu, Y.; Liu, Y.; Yan, P.; Liu, J.; Tang, J. Recent advances in synthetic methods and applications of silver nanostructures. *Nanoscale Res. Lett.* **2018**, *13*, 54.
(16) Fazio, E.; Gökce, B.; De Giacomo, A.; Meneghetti, M.; Compagnini, G.; Tommasini, M.; Waag, F.; Lucotti, A.; Zanchi, C. G.; Ossi, P. M.; Dell'Aglio, M.; D'Urso, L.; Condorelli, M.; Scardaci, V.; Biscaglia, F.; Litti, L.; Gobbo, M.; Gallo, G.; Santoro, M.; Trusso, S.; Neri, F. Nanoparticles Engineering by Pulsed Laser Ablation in Liquids: Concepts and Applications. *Nanomaterials* **2020**, *10*, 2317.
(17) Kim, M.; Osone, S.; Kim, T.; Higashi, H.; Seto, T. Synthesis of Nanoparticles by Laser Ablation: A Review. *KONA Powder and Part. J.* **2017**, *34*, 80−90.
(18) Bapat, M. S.; Singh, H.; Shukla, S. K.; Singh, P. P.; Vo, D-V.N.; Yadav, A.; Goyal, A.; Sharma, A.; Kumar, D. Evaluating green silver nanoparticles as prospective biopesticides: An environmental standpoint. *Chemosphere* **2022**, *286*, No. 131671.
(19) Skladanowski, M.; Golinska, P.; Rudnicka, K.; Dahm, H.; Rai, M. Evaluation of cytotoxicity, immune compatibility, and antibacterial activity of biogenic silver nanoparticles. *Med. Microbiol Immunol* **2016**, *205*, 603−613.
(20) Chikkanna, M. M.; Neelagund, S. E. Effect of Sheep and Goat Fecal Mediated Synthesis and Characterization of Silver Nanoparticles (AgNPs) and Their Antibacterial Effects. *J. Nanofluids* **2018**, *7*, 309−315.
(21) Ali, A.; Ovais, M.; Cui, X.; Rui, Y. K.; Chen, C. Safety Assessment of Nanomaterials for Antimicrobial Applications. *Chem. Res. Toxicol.* **2020**, *33*, 1082−1099.
(22) Ivask, A.; ElBadawy, A.; Kaweeteerawat, C.; Boren, D.; Fischer, H.; Ji, Z.; Chang, C. H.; Liu, R.; Tolaymat, T.; Telesca, D.; Zink, J. I.; Cohen, Y.; Holden, P. A.; Goodwin, H. A. Toxicity Mechanisms in Escherichia coli for Silver Nanoparticles and Differ from Ionic Silver. *ACS Nano* **2014**, *8* (1), 374−386.
(23) Niedermeyer, W. Method and apparatus for production of uniformly sized nanoparticles. US 9 849 512, 2017.
(24) Hackley, V.; Clogston, J.*NIST-NCL Joint Assay Protocol, PCC-1: Measuring the Size of Nanoparticles in Aqueous Media Using Batch-Mode Dynamic Light Scattering*; NCI Hub: 2020, DOI: 10.17917/3F5S-6728.
(25) Bonevich, J.; Haller, W. *NIST-NCL Joint Assay Protocol, PCC-7: Measuring the Size of Nanoparticles Using Transmission Electron Microscopy*; NCI Hub, DOI: 10.17917/C7N7-N938.
(26) Miller, L.; Chappell, M. Nanomaterial Dispersion/Dissolution Characterization: Scientific Operating Procedure SOP-F-1. Environmental Laboratory, U.S. Army of Engineer Research and Development Center, Vicksburg, MS 39180−6199. ERDC/EL SR-16−1 May 2016. http://hdl.handle.net/11681/20316 (accessed Mar 23, 2023).
(27) Kennedy, A.; Hull, M.; Bednar, A.; Goss, J.; Bouldin, J.; Vikesland, P.; Steevens, J. Fractionating nanosilver: importance for determining toxicity to aquatic test organisms. *Environ. Sci. Technol.* **2010**, *44* (24), 9571−9577.

https://doi.org/10.1021/acsomega.3c07745
ACS Omega 2024, 9, 7891−7903